The Role of Xantphos in forming an Elusive dirhodium-η^1-allyl Intermediate in a Rh(II)-Catalyzed Allylic Alkylation: A Combined Computational and Experimental Study

Anubhav Goswami,[a] Romin Gogoi,[a] Arpita Panda,[b] Aakash Chandresh Sheth,[a]‡ and Garima Jindal*[a]

[a]Department of Organic Chemistry, Indian Institute of Science, Bangalore 560012 (India)

[b]Department of Inorganic and Physical Chemistry, Indian Institute of Science, Bangalore, 560012 (India)

‡Current address: ONGC Cambay Asset, Khambhat, Gujarat 388620 (India)

email: gjindal@iisc.ac.in

Abstract

The use of dirhodium tetracarboxylate catalysts in multicomponent reactions involving allylic alkylation has been a formidable challenge to synthetic chemists. A unique strategy by means of catalyst structure modification in the presence of an external ligand, Xantphos, has recently enabled their efficient use in one-pot reactions involving carbene insertion into X–H bonds followed by allylic alkylation. However, the origin of the novel reactivity and the mechanism of such reactions remains unclear. Herein, we report a combined computational and experimental mechanistic study to shed light on the ligand enabled catalyst structure modification and its implication in catalysis. This unique reactivity is enabled by the dissociation of an octanoate bridge driven by κ^2-Xantphos ligation to the dirhodium core of the catalyst. This, in turn, allows for the hitherto unknown oxidative addition with a Rh(II) catalyst resulting in a dirhodium-η^1-allyl species. For the first time, we confirm the presence of such a species in solution through *in situ* NMR and cyclic voltammetry experiments in line with DFT calculations. Alongside, we study the role of the base and solvent in generating the nucleophilic partner that can trap the electrophilic allylic species. This study is expected to guide future catalyst design including chiral variants for exploring newer modes of reactivity and selectivity using dirhodium catalysis.

1 Introduction

Dirhodium tetracarboxylate-based paddlewheel complexes have found widespread utility in the functionalization of X–H (X = N, O, S, C) bonds with impressive regio-, chemo-, and stereoselectivities.[1] The simple yet elegant two-component strategy has been further extended to MCRs (multicomponent reactions) where the reactive onium ylide intermediate traps an external electrophile. The capture of external electrophiles both in the form of Michael acceptors (prior to a delayed proton transfer) and electrophile transfer reagents or intermediates to yield valuable and diverse molecular scaffolds has been reported (Scheme 1).[2]

Despite the burgeoning success of dirhodium tetracarboxylate-based catalysts for X–H insertion reactions, the catalysts of choice for another class of reactions involving allylic alkylation via metal-allyl intermediates largely remain monorhodium and palladium-based.[3] This is due to the ease of formation of these intermediates through a facile oxidative addition process, which is typically not possible in the stable dirhodium tetracarboxylate architecture owing to the lack of two vacant adjacent coordination sites. Due to this, dirhodium tetracarboxylate-based catalysts are incapable of catalyzing the MCRs involving allylic reagents as electrophiles.[2k,l] This necessitates the use of two metal catalysts, one for the formation of the metal carbene and the other for that of the metal-allyl complex. In this context, the use of Rh and Pd has been a convenient strategy to form complex targets. However, an ideal scenario would be the use of single catalyst that can enable both carbene insertion followed by allylic alkylation or vice versa. Although monorhodium-based catalysts are also capable of X–H insertion reactions and can thereby in principle be used as the sole metal catalyst for MCRs,[4] they fail to catalyze the MCR involving allylic alkylation most likely due to their tendency to easily form the metal-allyl intermediate through oxidative addition and the subsequent allylic alkylation of the X–H based nucleophile, precluding the metal carbene formation and X–H insertion, and instead affording the X-allylated product.[5]

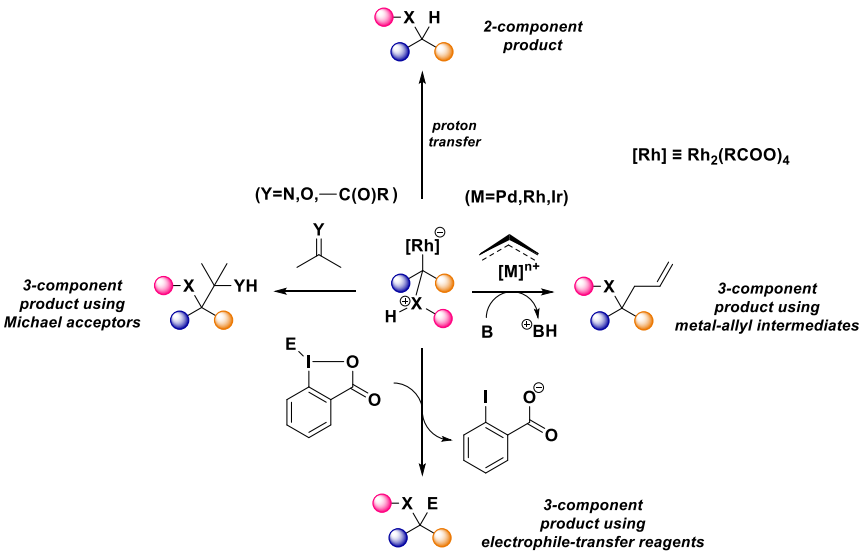

Scheme 1. Two- and three-component reactions catalysed by dirhodium carboxylates.

Despite the challenges discussed above, Wang and co-workers recently developed a MCR protocol for the construction of α-quaternary α-amino ester from an α-diazoester, amine, and allylic compound, involving a dirhodium tetracarboxylate/Xantphos-catalyzed carbene insertion and allylic alkylation relay (Scheme 2).[5] The unique reactivity was a result of the combination of different factors that include the nature of the catalyst, external ligand, base, and solvent. Their synthesis design was based on the possible modification of the catalyst in the presence of the external Xantphos ligand where the choice of the solvent and base also played a crucial role. The modification of dirhodium catalysts in different ways has enabled newer reactivity in several other reactions. For instance, chiral carboxylate ligands have been incorporated into the catalyst framework for the development of asymmetric X–H insertion reactions.[6] There have also been a number of attempts to tune the reactivity of dirhodium-based catalysts by the use of external and tethered axial ligands without modifying the paddlewheel framework.[7] Although the use of external chiral ligands in this aspect has only resulted in modest enantioselectivities so far, the differential reactivities are of immense importance.[7b] In the work by Wang and coworkers, it was hypothesized that the external Xantphos ligand drives the dissociation of one of the carboxylate ligands. This is turn provides vacant adjacent sites necessary for the oxidative addition of the allyl substrate resulting in the formation of a hitherto unreported dirhodium-η^1-allyl species, which is postulated to serve as the active allylating agent in the reaction (Scheme 3). However, they were able to detect neither the cationic complex nor the Rh-allyl species. Numerous similar reports of carbene insertion and allylic alkylation relay utilizing this strategy have followed thereafter,[8] making it necessary to establish the mechanistic details of this reaction. Recently, this strategy of ligand induced dirhodium catalyst modification has also been applied to a carbonyl arylation reaction involving external chiral ligands.[9] This arylation reaction, supposedly proceeding via a similar modified catalyst, provides the motivation for developing asymmetric reactions for MCRs as well. Since there are no experimental or computational reports on the mechanistic front for this intriguing MCR, in this work, we attempt to delineate its mechanism and the key species involved via computational and experimental studies.

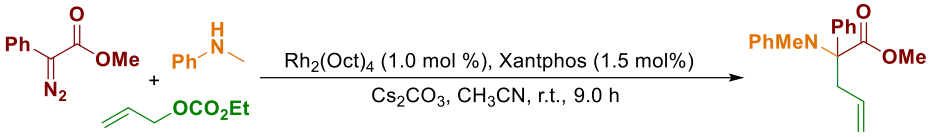

Scheme 2. General scheme for the synthesis of α-quaternary α-amino ester.

The work under investigation involves a relay pathway where the N–H insertion product (an α-amino ester) is formed, exits the catalytic cycle, and enters the subsequent catalytic cycle for allylic alkylation (Scheme 3). As shown by Wang and co-workers,[5] when the N–H insertion product is subjected to the standard reaction conditions, the α-quaternary α-amino ester is formed in high yield, thus confirming the relay nature of this MCR. This relay reactivity is different from the other MCRs where the ylide/enol intermediate traps the external electrophile. Under these circumstances, there is competition between the formation

of the two- and three-component products. However, in the reaction under investigation, the two-component product is first formed, which then undergoes further reaction. In the absence of the Xantphos ligand, the reaction stops at the N–H insertion product, thereby indicating that the ligand is essential for the subsequent allylic alkylation. At the same time, deviations in the solvent and base also significantly affected the yield of the α-quaternary α-amino ester. We therefore set out to first investigate the role of Xantphos in the allylic alkylation of the α-amino ester. The primary goal is to establish the nature of the electrophilic and nucleophilic species participating in this allylic alkylation reaction. Our study provides the first explanation for the unique reactivity of the dirhodium/Xantphos system. We confirm our mechanistic model obtained through DFT calculations using *in situ* NMR and CV experiments.

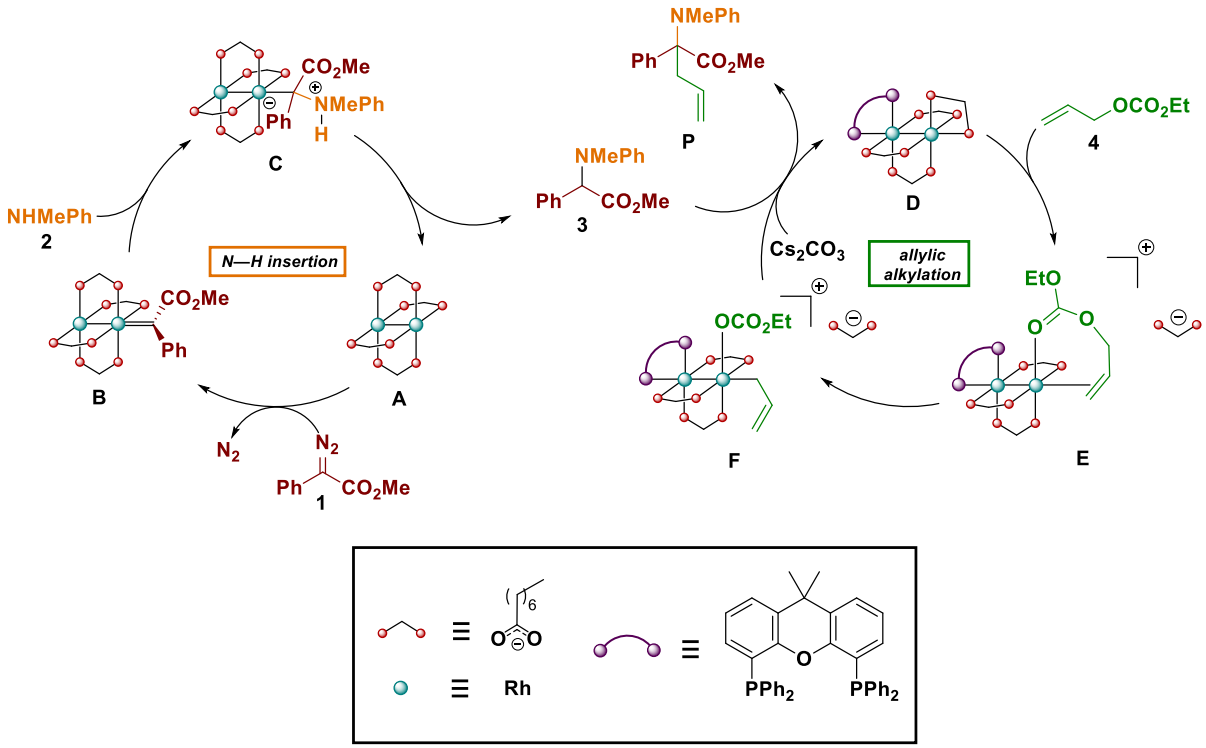

Scheme 3. Proposed mechanism for dirhodium tetracarboxylate/Xantphos-catalyzed carbene insertion and allylic alkylation relay.

2 Results and Discussion

2.1 Search for the active catalyst

We begin our study by looking at the different possibilities for the most stable active form of the catalyst (Figure 1) at the $SMD_{(acetonitrile)}$/B3LYP-D3(BJ)/6-311++G(d,p),SDD(Rh,Cs)//B3LYP-D3(BJ)/6-31G(d,p),SDD(Rh,Cs) level of theory. In the absence of the external Xantphos ligand, the complex **A5** with one molecule each of Cs_2CO_3 coordinated axially to the two ends of dirhodium tetracarboxylate catalyst was found to be most stable. However, this diaxial mode of coordination blocks both ends of the catalyst and

prevents subsequent reactions, *viz.* N–H insertion and Rh association for allylic alkylation due to lack of any reactive sites and an over-stabilized complex, leading to a dead end. This phenomenon has been previously studied by Pirrung and co-workers for dirhodium tetracarboxylate catalyzed C–H insertion.[10] A kinetic treatment in their report using different axial ligands revealed that axial ligand coordination in general slowed down the insertion reaction and that bis-coordination leads to a catalytic dead end. Therefore, the complex with Cs_2CO_3 coordinating to one of the axial sites of the catalyst **A4** is most likely the active form of the catalyst in the absence of Xantphos.

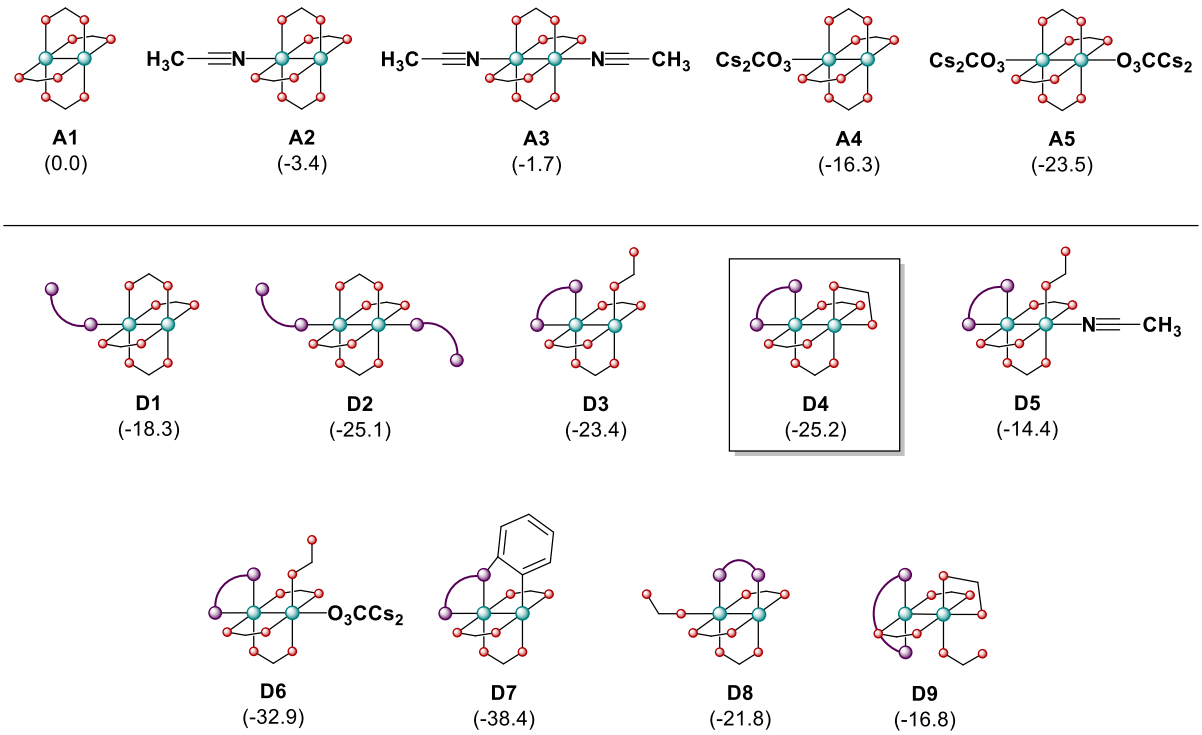

Figure 1. Possible active catalysts (relative free energies are in kcal mol^{-1}).

In the presence of Xantphos, the κ^1-mode of coordination of Xantphos to the catalyst (**D1**) leads to a stabilization of 18.3 kcal mol^{-1}. The bis-coordination of two Xantphos in the κ^1-mode to the two axial sites (**D2**) leads to a stabilization of 25.1 kcal mol^{-1}. However, this bis-coordinated form cannot function as the active catalyst as it blocks both the reactive axial sites, as discussed previously in the case of Cs_2CO_3 coordination. These two geometries correspond to the crystal structures reported by Wang and co-workers.[5] A third crystal structure reported by this group (**D7**) provides indirect evidence for the κ^2-Xantphos coordination to one of the rhodium centres by the dissociation of an octanoate bridge (**D4)**, and they hypothesize this to be the active form of the catalyst.[5,12] Recent reports in dirhodium catalysis have also invoked this hypothesis to explain the catalytic activity in their reactions.[8,9] This complex **D4**, with the dissociated bridge octanoate now coordinating in a κ^2 fashion to the second rhodium centre, was found to be stabilized by 25.2 kcal mol^{-1} (the coordination of a Cs_2CO_3 molecule to the opposite axial site **D6** was found to be further

stabilizing by 7.7 kcal mol^{-1}, but was discarded as a dead end following the same reasoning as above).

With the active catalytic species in the absence and presence of the external Xantphos ligand established, we attempted to study the allylic alkylation of the N–H insertion product, *i.e.*, the α-aminoester **3** (Scheme 3). The mechanism of X–H (X = N, O, S, C) insertion reactions catalyzed by dirhodium tetracarboxylate and other transition metal complexes have been well studied computationally and reported to proceed through metallocarbene, **B** formation from diazoesters followed by a nucleophilic attack to yield the ylide, **C** and subsequent proton transfer to yield the X–H insertion product, **3** (Scheme 3).[13] Therefore, the first catalytic cycle for the N–H insertion reaction leading to the α-aminoester, **3** has not been investigated computationally in this work. The nucleophile in this process is likely an enolate formed from the deprotonation of the α-proton from the α-aminoester by the Cs_2CO_3. The enolization of the α-aminoester by Cs_2CO_3 in acetonitrile was confirmed by 42% deuterium incorporation using D_2O, as verified from ^{1}H NMR (see Supporting Information Section C). This enolization was calculated to proceed with a free energy barrier of 7.8 kcal mol^{-1} and 8.9 kcal mol^{-1} to form (*E*)-enolate and (*Z*)-enolate respectively, thereby confirming the feasibility of such a process. All calculations presented hereafter have considered the kinetically more feasible (*E*)-enolate (calculations with the (*Z*)-enolate show similar trends, see Supporting Information Figure S1 and Figure S2 for details).

2.2 Reaction pathways in absence of Xantphos

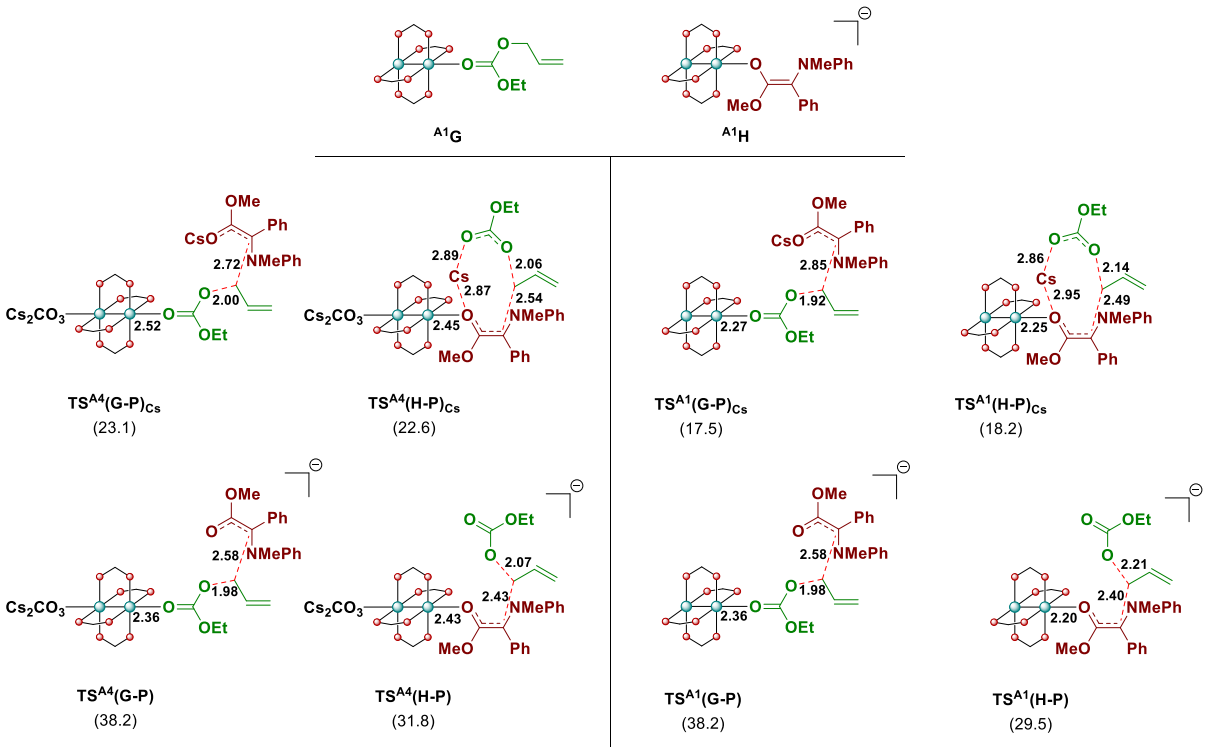

Figure 2. Transition states and the relative free energies (kcal mol^{-1}) with respect to the catalytic species **A5** (left) and **A1** (right) in the absence of Xantphos.

In the absence of Xantphos, we considered a Rh-associated enolate (**H**) as a possible intermediate effecting a nucleophilic attack on allyl carbonate. We also speculated the external attack of a nucleophile on a Rh-associated allyl carbonate (**G**). However, whether the nucleophile (generated by a proton abstraction from the N–H insertion product) is a Cs-enolate or a Cs-free enolate is dubious. The nucleophilic attack of the Cs-enolate on the Rh-associated allyl carbonate $\mathbf{TS^{A4}(G\text{-}P)_{Cs}}$ was found to have a barrier of 23.1 kcal mol^{-1}, and the nucleophilic attack of the Rh-associated Cs-enolate on allyl carbonate $\mathbf{TS^{A4}(H\text{-}P)_{Cs}}$ to have a barrier of 22.6 kcal mol^{-1} (Figure 2, left). Such low free energy barriers indicate a facile reaction at room temperature (for reference, N_2 expulsion for metallocarbene formation, the typical rate-determining step for the N–H insertion pathway, has barriers of 22.3 kcal mol^{-1} and 14.7 kcal mol^{-1} with and without Xantphos, respectively, Figure S3), in stark contrast to experimental results where no allylic alkylation is observed in the absence of Xantphos. Previous studies on the extent of ion-pairing in alkali enolates have revealed a decreasing trend of ion-pairing going from Li^+ to Na^+ to K^+ (log K_{assoc} = 4.6, 3.3, 2.3 respectively for diethyl malonate in DMSO) showing an inverse relation with cation size.[14] Based on the much larger size of the Cs^+ cation and the polarity of the solvent, the Cs-enolate is expected to be in the completely solvent-separated form. In fact, the so-called "cesium effect" used in justifying the enhanced reactivity of cesium salts, cesium carbonate in particular, as compared to other alkali metal analogues is often explained in terms of the higher solubility of these salts on account of their greater solvation.[15] Thus, incorporating a Cs-enolate species in our DFT calculations might be incorrect and leads to the unrealistically low free energy barriers stated above, causing us to exclude the Cs-bound enolate from our calculations. Therefore, expecting a similar behaviour of Cs in the current work, too, we, therefore incorporate the Cs-free enolate as the nucleophilic species in this reaction and find the nucleophilic attack of the enolate on the Rh-associated allyl carbonate $\mathbf{TS^{A4}(G\text{-}P)}$ to have a barrier of 38.2 kcal mol^{-1} and that of the Rh-associated enolate on allyl carbonate $\mathbf{TS^{A4}(H\text{-}P)}$ to have a barrier of 31.8 kcal mol^{-1} (Figure 2, left). The reaction pathways corresponding to the catalyst without axial Cs_2CO_3 coordination were also studied and found to have a similar trend of free energy barriers (Figure 2, right).

2.3 Reaction pathways in presence of Xantphos

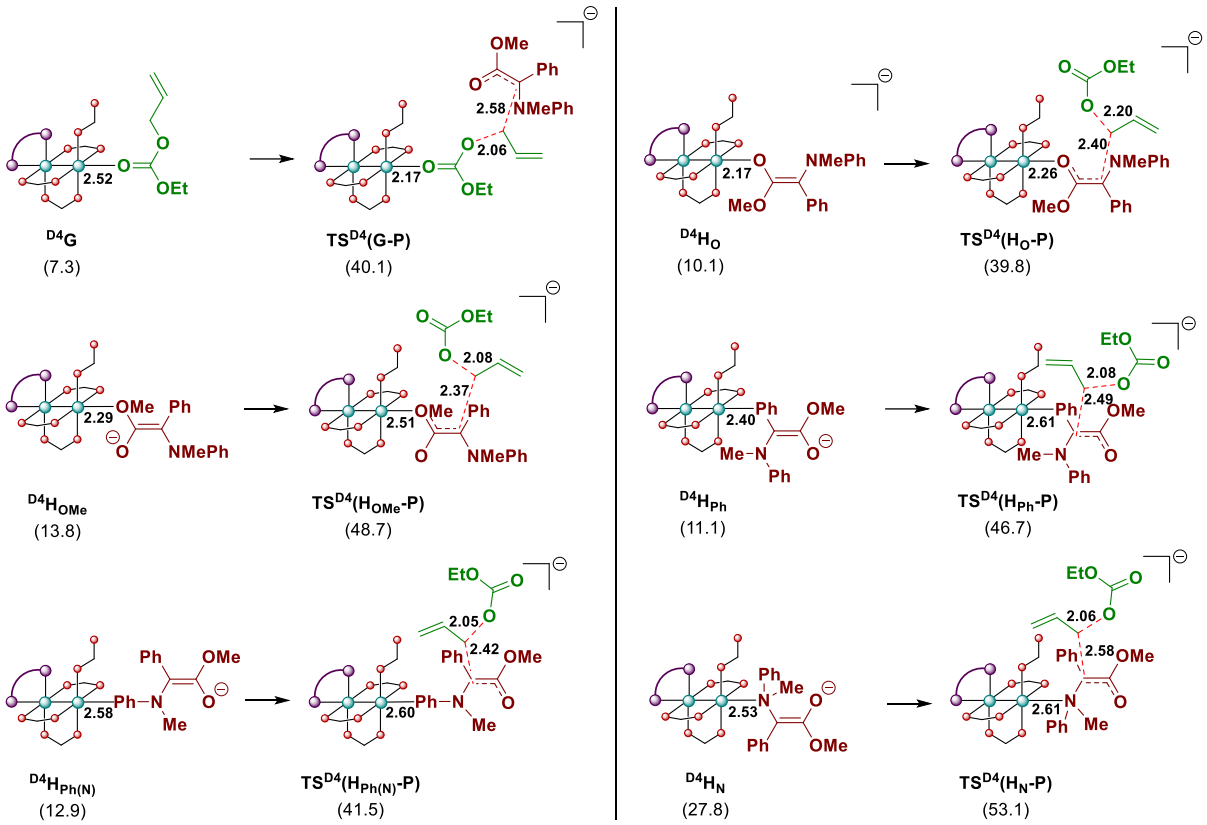

Figure 3. Intermediates and transition states and their associated free energies for pathways involving Rh-associated allyl carbonate and Rh-associated enolates in presence of Xantphos (free energies relative to catalyst **D4** are given in kcal mol^{-1}).

Having rationalized the reactivity in the absence of Xantphos, we investigated the potential reaction pathways in the presence of Xantphos (Figure 3). As discussed in Section 3.1, complex **D4** with a κ^2-Xantphos coordination is considered to be the active form of the catalyst[16] and all relative free energies are hereafter referenced to it. As the oxidative addition pathway[5] has no literature precedence in the context of dirhodium catalysis, we looked at the possibility of a Rh-associated enolate as an intermediate with a subsequent nucleophilic attack on allylic carbonate, but each of these pathways **TS^{D4}(Hx-P)** (where **X** denotes the enolate binding site) was calculated to have a preventively high free energy barrier. The nucleophilic attack of the enolate on the Rh associated allyl carbonate **TS^{D4}(G-P)** was also found to have a very high barrier. (Note: In both the above possibilities, incorporating a Cs-enolate or a Rh-associated Cs-enolate as the nucleophile yields much lower barriers (Figure S5), but must be disregarded in accordance with our previous justification). The possibility of an allyl transfer from a Rh-associated allyl carbonate to the neighboring κ^1-octanoate (Figure S6) was also excluded based on high energy transition states.

2.4 The oxidative addition pathway

Wang and co-workers have hypothesized the complete dissociation of the octanoate ligand from the κ^2-Xantphos dirhodium tetracarboxylate active catalyst along with a concomitant association of the allyl carbonate to the cationic dirhodium species (Scheme 3).[5,16] Previous reports involving dirhodium carboxylate catalysts with and without external ligands have also

hypothesized the complete dissociation of a carboxylate ligand[17] although the external ligand-free version has been challenged.[18] We calculated the allyl carbonate associated dirhodium cation/octanoate ion pair **E** to be destabilized by 15.8 kcal mol^{-1} (Figure 4). However, the calculation of charged species, especially for an ion pair such as this, by even state-of-the-art DFT methods, has been previously noted to have errors up to five kcal mol^{-1} in general[19] and more than seven kcal mol^{-1} in certain cases.[20] In order to get a more accurate estimate, as outlined in previous protocols,[20] we tried incorporating up to four explicit solvent (MeCN) molecules without seeing any additional stabilization. A solvent phase optimization at the $SMD_{acetonitrile}$/B3LYP-D3(BJ)/6-311++G(d,p),SDD(Rh,Cs)//$SMD_{acetonitrile}$/B3LYP-D3(BJ)/6-31G(d,p),SDD(Rh,Cs) level of theory led to a reduced free energy of 14.1 kcal mol^{-1}.[21]

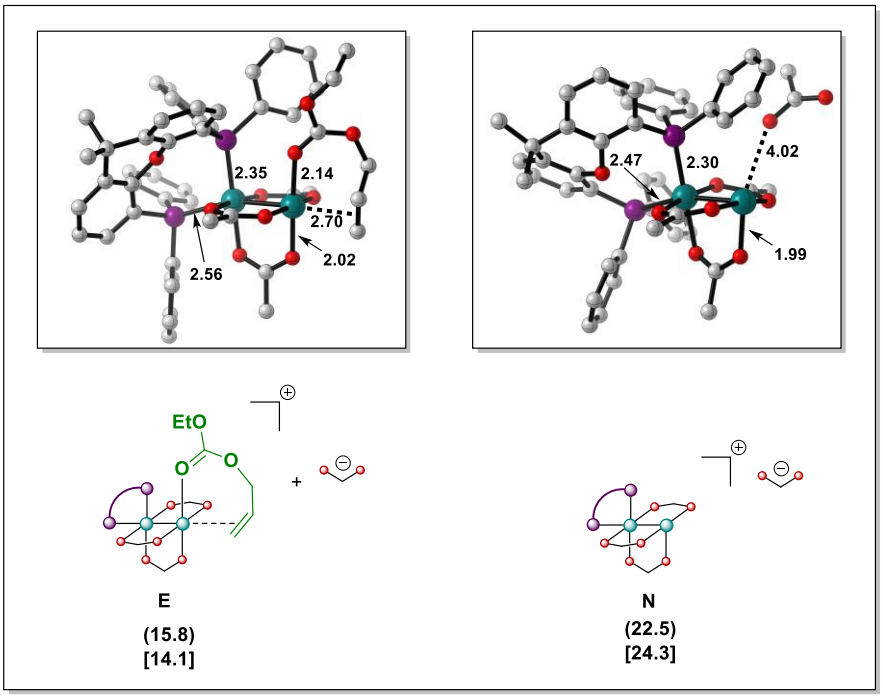

Figure 4. Optimized geometries for the ion pairs following the complete octanoate dissociation with and without allyl carbonate association (free energies in parenthesis correspond to the gas-phase optimized geometry relative to **D4**, free energies in parenthesis correspond to the solvent-phase optimized geometry relative to **D4**, given in kcal mol^{-1}).

To ascertain the existence of such an intermediate, we therefore resorted to experimental methods. We first performed *in situ* ^{1}H NMR experiments (Figure 5) under inert conditions. Upon addition of the commercially available allyl chloride to a mixture of dirhodium tetraacetate and Xantphos in acetonitrile-*d3*, we observed an allyl species distinct from the allyl chloride to be present in 16-20% relative yield (Figure 5(b)), which is absent in the control experiment without Xantphos (Figure 5(a)). Closer inspection revealed the allylic protons in the new allyl species to be in the form of a doublet of doublet of doublets at 4.41 ppm likely due to $^{3}J_{H\text{-}H}$ and $^{2}J_{H\text{-}Rh_1}$, and $^{3}J_{H\text{-}Rh_2}$ coupling corresponding to $^{103}Rh_2$–$^{103}Rh_1$ (J = 4.9 Hz, 6.9 Hz, 16.9 Hz) (Figure 5(c)), confirming the presence of a dirhodium-η^1-allyl species in solution.

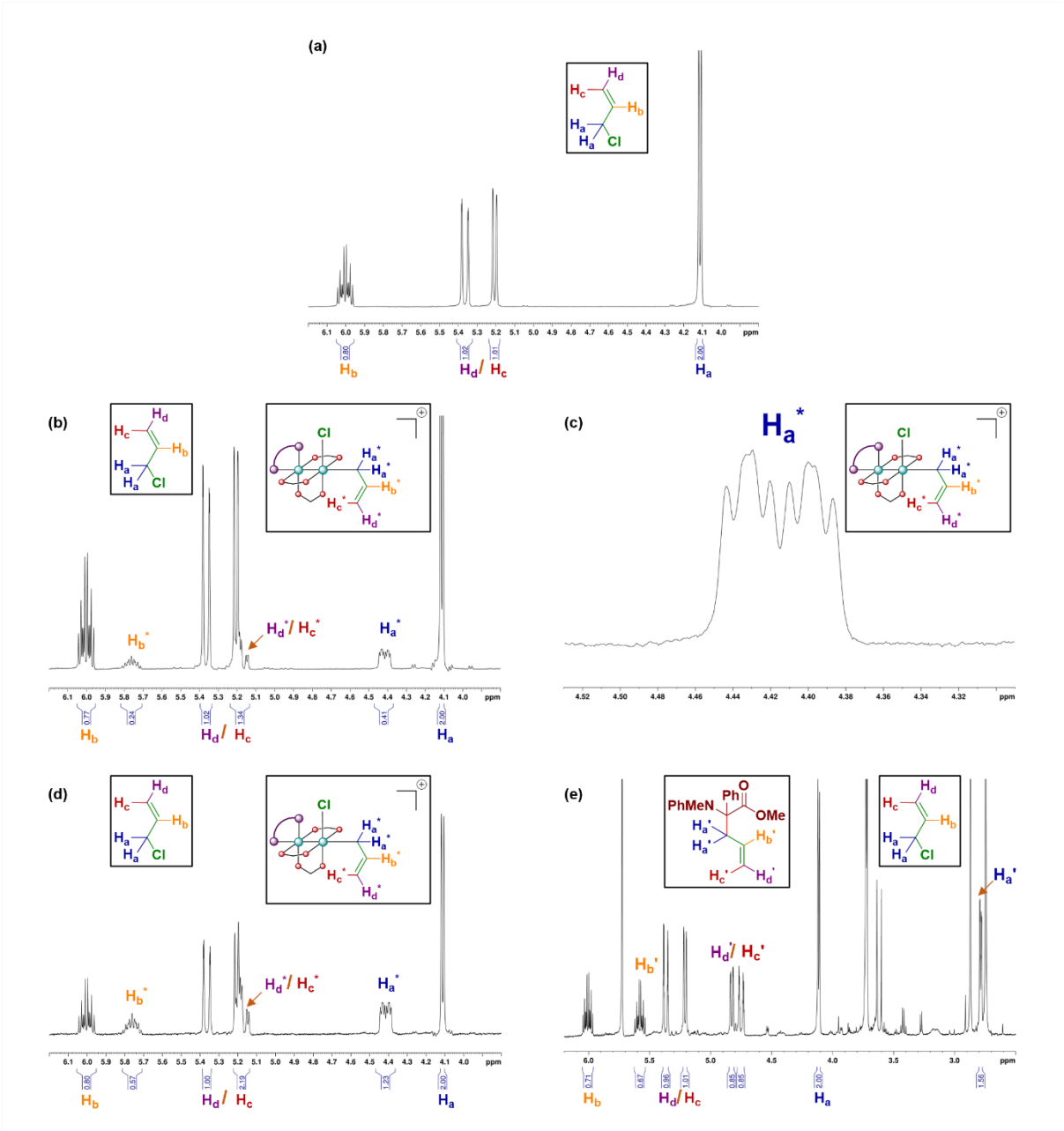

Figure 5. *in situ* ^{1}H NMR spectra of (a) equimolar mixture of dirhodium tetraacetate and allyl chloride (b) equimolar mixture of dirhodium tetraacetate, Xantphos, and allyl chloride (c) spectrum (b) magnified to focus on the doublet of doublet of doublet at 4.41 ppm (d) equimolar mixture (stirred overnight) of dirhodium tetraacetate, Xantphos, allyl chloride, and cesium carbonate (1.5 equiv) (e) 1 equiv of α-amino ester added to the solution in (d); all in acetonitrile-*d3*. **Note:** Although the cartoon representation adopted here is the same as before, the rhodium complex being used here is dirhodium tetraacetate and not dirhodium tetraoctanoate.

This indicates the oxidative addition of the allylating agent (allyl carbonate, allyl chloride, etc.) across the rhodium centre to which it is associated (in intermediate **E**) to form the detected dirhodium-η^1-allyl intermediate. Encouraged by this observation, we attempted to computationally examine the pathway of formation of this dirhodium-η^1-allyl intermediate

(Figure 6). As the energy penalty of the ion pair **E** with respect to the neutral system cannot be accurately captured by our calculations (discussed above), we consider all subsequent free energies relative to this intermediate. The oxidative addition pathway **TS(E-F)** was found to be most favourable, possessing an activation free energy barrier of 17.2 kcal mol^{-1} with respect to the intermediate **E**, leading to the dirhodium-η^1-allyl intermediate **F** with a free energy of 14.9 kcal mol^{-1} with respect to **E** (calculations using dirhodium tetraacetate and allyl chloride, which are used for all experiments, show similar trends; Figure S7). It must be noted here that the Rh "enyl" intermediate **K** (proposed by Evans and co-workers[22] in the case of Rh(I)/Rh(III) catalysis) was calculated to be 28.7 kcal mol^{-1} higher in energy than the dirhodium-η^1-allyl intermediate **F** and was therefore discarded as a possible intermediate. Additionally, the direct Rh-allylation by allyl carbonate (formally, a *nucleophilic displacement* or the first step of a stepwise oxidative addition pathway; Figure S6) was calculated to have a preventively high barrier. For the sake of completeness, we also considered the exchange of the non-bridging octanoate ligand with the enolate and a subsequent inner sphere allylic alkylation by a Rh-associated allyl carbonate but found these pathways to possess insurmountable barriers (Figure S8).

In order to confirm that the oxidative addition pathway is indeed taken, CV (cyclic voltammetry) measurements were performed under inert conditions in acetonitrile with tertbutylammonium hexafluorophosphate as the supporting electrolyte (see Section **2.3** for details). Dirhodium tetraacetate showed the reported reversible one-electron oxidation/reduction wave at 1.18 V (Figure 7(a) and 7(b)),[23] while Xantphos exhibited three separate quasireversible oxidation/reduction waves at 1.13 V, 1.48 V, and 1.98 V (Figure S9). When dirhodium tetraacetate and Xantphos were taken together in solution, a nearly irreversible hump near 0.94 V was observed and the wave corresponding to one-electron oxidation/reduction of dirhodium tetraacetate turned quasireversible without any shift in potential (Figure 7(c) and 7(d)). This further supported the complexation of Xantphos with dirhodium tetraacetate. Upon adding allyl chloride along with dirhodium tetraacetate and Xantphos in solution, new quasireversible reduction/oxidation waves near -1.38 V and -1.58 V were observed (Figure 7(e) and 7(f)), likely corresponding to the two-electron reduction of the oxidative addition product, i.e., $[Rh_2]^{6+}$ to $[Rh_2]^{4+}$. These waves were absent in all control experiments (Figure S9). Thus, it was confirmed that the product observed through *in situ* ^{1}H NMR results from oxidative addition.

Following the verification of the existence of the dirhodium-η^1-allyl intermediate and establishing the pathway of its formation, we turned to examine its fate the in presence of the α-amino ester. We again performed the *in situ* ^{1}H NMR of a mixture of dirhodium tetraacetate, Xantphos, cesium carbonate, and allyl chloride in acetonitrile-*d3*, shaking the solution overnight to ensure maximum formation of the desired dirhodium-η^1-allyl complex. The ^{1}H peaks corresponding to the dirhodium-η^1-allyl species were reproduced, indicating 38-40% relative yield (Figure 5(d)). Upon addition of the α-amino ester, the above-mentioned peaks disappear completely, and a new set of allyl peaks appear, corresponding to the product, i.e., α-quaternary α-amino ester (Figure 5(e)). This further validates the idea that this dirhodium-η^1-allyl intermediate, in fact, leads to product formation by the nucleophilic attack of the deprotonated α-amino ester.

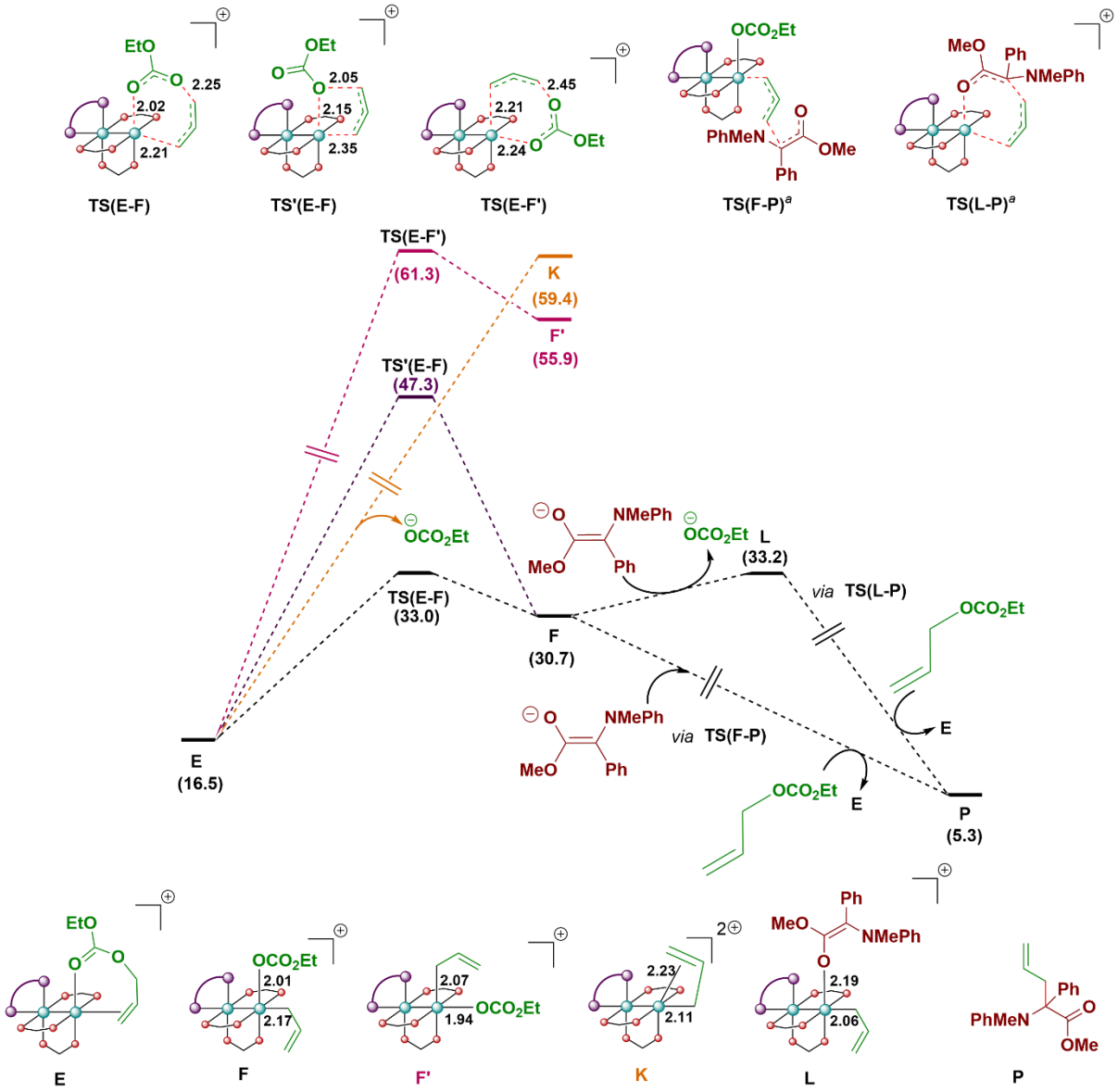

Figure 6. Reaction profile for the possible oxidation pathways of allyl carbonate (free energies relative to **D4** are given in kcal mol^{-1}). [a]**TS(F-P)** and **TS(L-P)** are only representative; they could not be located. However, **TS(F-P)** is expected to be barrierless.

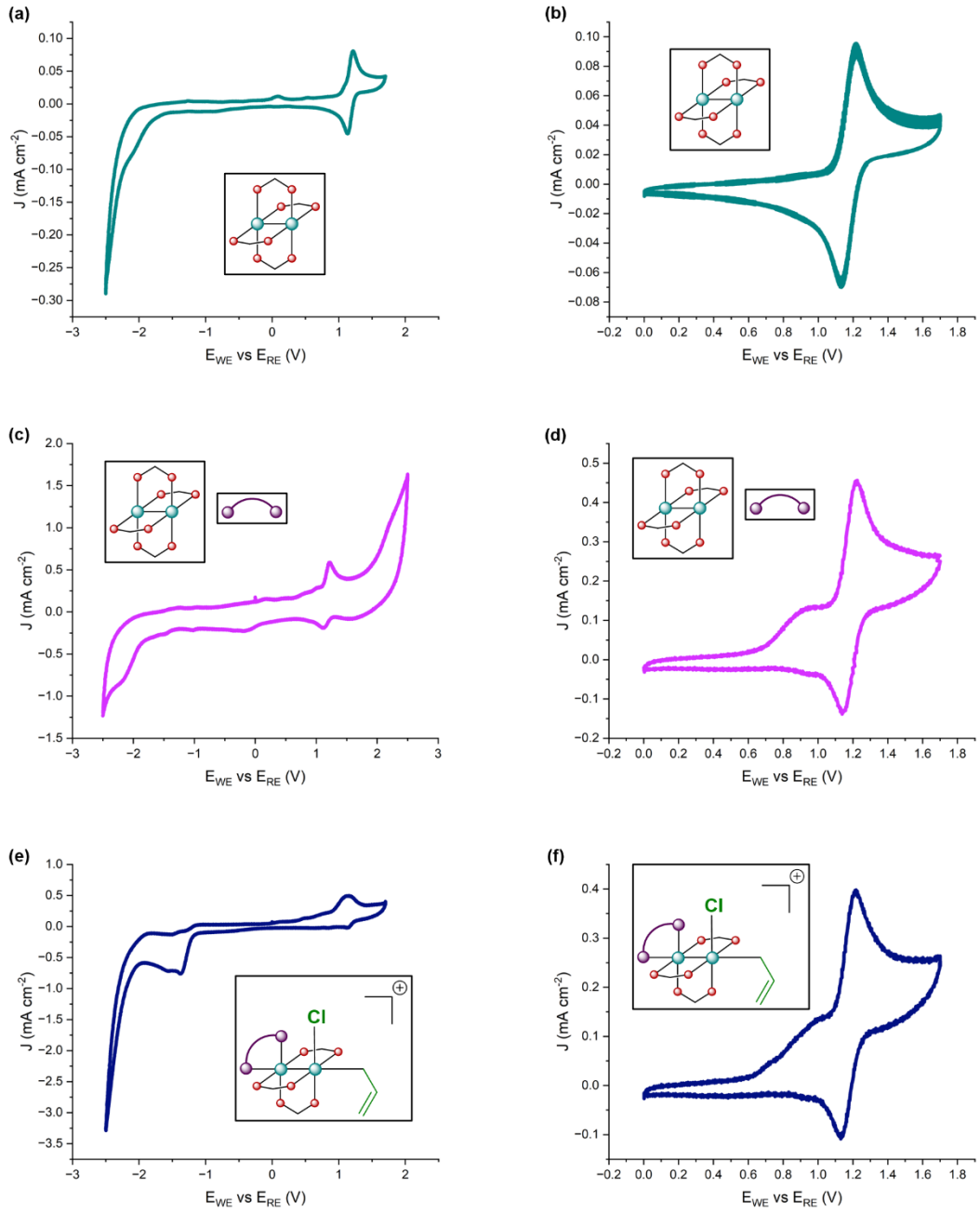

Figure 7. CV of (a), (b) dirhodium tetraacetate (c), (d) equimolar mixture of dirhodium tetraacetate and Xantphos (e), (f) equimolar mixture of dirhodium tetraacetate, Xantphos, and allyl chloride (1.25 mM in 0.1 M tetrabutylammonium hexafluorophosphate in CH_3CN; scan rate = 0.1 V s^{-1}). **Note:** Although the cartoon representation adopted here is the same as before, the rhodium complex being used here is dirhodium tetraacetate and not dirhodium tetraoctanoate.

Two potential pathways for allylic alkylation of the α-amino ester through this dirhodium-η^1-allyl species are most likely (Figure 6) – (1) the external nucleophilic attack of the enolate, here an S_N2'-like pathway via **TS(F-P)** is likely favoured over an S_N2-like pathway, as indicated by the deuterium labelling experiments by Wang and co-workers[5] as well as

previous reports for rhodium based allylic alkylation reacitons;[24] (2) the exchange of the κ^1-octanoate with the enolate (**L**) followed by a reductive elimination via **TS(L-P)** to yield the α-quaternary α-amino ester. However, numerous attempts to locate the transition states for both the S_N2'-like and reductive elimination pathways were unsuccessful. A previous DFT study by Sunoj and co-workers[25] indicates a nearly barrierless allylic alkylation transition state from a rhodium-η^3-allyl intermediate. We attempted to generate the potential energy surface for the S_N2'-like pathway using a reduced system (acetate in place of octanoate and two trimethyl phosphine molecules in place of Xantphos), but no saddle point was seen in the relaxed energy scan (Figure 8), indicating a nearly barrierless transition state for this reaction.

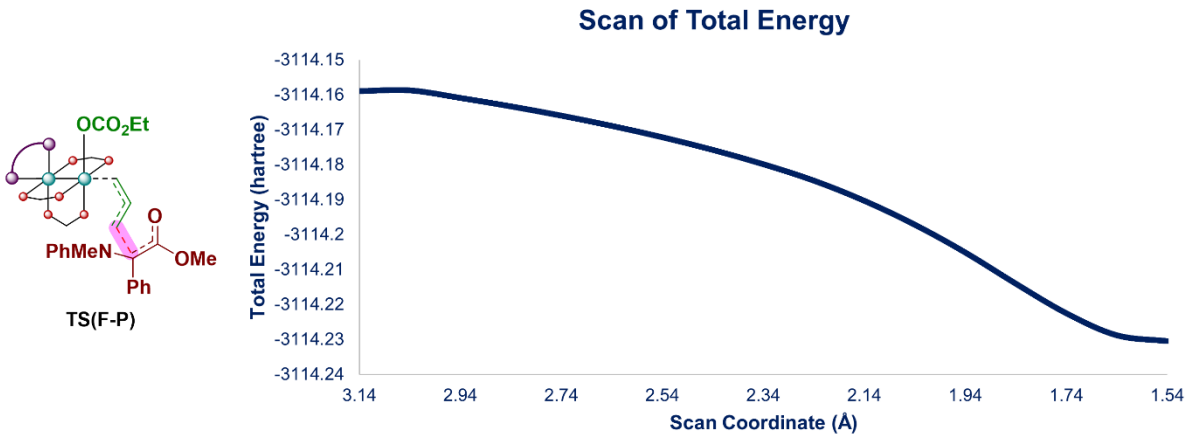

Figure 8. 1-dimensional Relaxed Potential Energy Surface (PES) scan. The distance being varied is highlighted in the representative **TS(F-P)**. Scan coordinate is in angstroms and Total Energy is in hartree.

3 Conclusion

In this work, we have unraveled the mechanistic possibilities for a dirhodium tetracarboxylate/Xantphos-catalyzed carbene insertion and allylic alkylation relay. Through computational studies, *in situ* NMR, and cyclic voltammetry experiments, we confirmed the existence of a dirhodium-η^1-allyl species as a reactive intermediate in this reaction. We have discussed the reactivity of this allylic species with nucleophilic components, with the Cs-free enolate species determined to be the probable nucleophile in solution. Furthermore, our combined study sheds light on the individual roles of the Xantphos ligand, the Cs_2CO_3 base, and the polar solvent. The ability of Xantphos to completely dissociate a carboxylate bridge, thereby bringing this interesting mechanistic paradigm into the picture, is expected to have serious implications in inducing new modes of reactivity utilizing dirhodium tetracarboxylate catalysts. Confirmation of the κ^2-Xantphos dirhodium tetracarboxylate active catalytic species is anticipated to pave the way for utilizing chiral bulky external ligands for efficient stereoinduction at the axial position. Recent reports on the use of chiral bisphosphine ligands such as DIOP[8b] and Josiphos[9] in dirhodium-catalyzed transformations illustrate this through good to excellent enantioselectivities for allylic alkylation and carbonyl addition respectively.

This κ^2-mode of coordination is therefore expected to serve as a launchpad for the development of asymmetric reactions for achieving challenging transformations.

4 Methods

4.1 Computational Details

All calculations were done using Gaussian 16 suite of quantum chemical programs.[26] The hybrid density functional B3LYP[27] along with the D3(BJ) version of Grimme's dispersion correction was used for geometry optimization with 6-31G(d,p) basis set[28] for all atoms except Rh and Cs. For Rh and Cs, the SDD basis set with effective core potential (SDD) was chosen.[29] The stationary points were characterized by frequency calculations. The transition states were verified by the unique imaginary frequency calculation concerning the desired reaction coordinate. Moreover, intrinsic reaction coordinate (IRC) calculations were carried out to verify the correctness of the transition states obtained. For all stationary points single calculations were performed using higher basis set 6-311++g(d,p) and all sorts of dispersion interaction were taken into account using the D3(BJ) version of Grimme's dispersion correction.[30] To take into the effect of solvent the keyword SCRF is used which performs calculations in the presence of a solvent by placing the solute in a cavity within the solvent reaction field, and herein solvent model density (SMD) with acetonitrile (ε = 35.688) was used.[31] The ZPE (zero point energy), thermal, and entropic corrections obtained at 298.15 K and 1 atm pressure calculated in the gas phase at B3LYP-D3(BJ)/6-31G(d,p),SDD(Rh,Cs) level of theory were added to the 'bottom-of-the-well' energies obtained from single point calculations at the $SMD_{acetonitrile}$/B3LYP-D3(BJ)/6-311++G(d,p),SDD(Rh,Cs) level of theory. All the values mentioned in this work, unless mentioned otherwise, correspond to free energies obtained at the $SMD_{acetonitrile}$/B3LYP-D3(BJ)/6-311++G(d,p),SDD(Rh,Cs)//B3LYP-D3(BJ)/6-31G(d,p),SDD(Rh,Cs) level of theory.

4.2 NMR Spectroscopy

^{1}H NMR spectra were measured on an Avance Bruker 500 MHz NMR spectrometer at RT. Chemical shifts were reported in ppm with respect to $SiMe_4$ by referencing the solvent peak to $SiMe_4$. All *in situ* NMR experiments were set up inside an N_2-filled glove box using an airtight screw cap NMR tube.

4.3 Cyclic Voltammetry

Cyclic Voltammetry was performed using 12 mL dried and distilled acetonitrile solutions containing 0.1 M tertbutylammonium hexafluorophosphate with 0.00125 M analyte under a nitrogen atmosphere. The electrodes consisted of a glassy carbon working electrode, a Pt wire counter electrode, and an Ag/AgCl reference electrode. Measurements were taken using a Biologic SP-150 potentiostat. Prior to the measurement, all components of the analyte were taken inside the electrochemical cell and degassed before introducing it to nitrogen flow in order to ensure completely inert conditions.

4.4 Synthesis

The α-amino ester (**3**) was prepared according to a previously reported procedure.[32] All other chemicals were purchased commercially and used without further purification.

Acknowledgements

G. J. acknowledges the research grant (SPG/2021/003445) from Science and Engineering Research Board (SERB). A. G. thanks the Dept. of Science & Technology, Govt. of India, for the KVPY fellowship. We are grateful to Prof. Balaji Rao Jagirdar, Prof. Santanu Mukherjee, and Dr. Veerabhadrarao Kaliginedi for generously allowing us to use their experimental labs and helpful discussions. We thank Ms. Kamla Devi Netam and Mr. Arko Seal for aiding in a portion of the experiments. We thank SERC, IISc for computing time.

References

(1) (a) Davies, H. M. L.; Manning, J. R., Catalytic C–H functionalization by metal carbenoid and nitrenoid insertion. *Nature* **2008**, *451*, 417-424. (b) Doyle, M. P.; Forbes, D. C., Recent Advances in Asymmetric Catalytic Metal Carbene Transformations. *Chem. Rev.* **1998**, *98*, 911-936. (c) Boyar, E. B.; Robinson, S. D., Rhodium(II) carboxylates. *Coord. Chem. Rev.* **1983**, *50*, 109-208. (d) Doyle, M. P.; Duffy, R.; Ratnikov, M.; Zhou, L., Catalytic Carbene Insertion into C−H Bonds. *Chem. Rev.* **2010**, *110*, 704-724. (e) Zhu, S.-F.; Zhou, Q.-L., Transition-Metal-Catalyzed Enantioselective Heteroatom–Hydrogen Bond Insertion Reactions. *Acc. Chem. Res.* **2012**, *45*, 1365-1377. (f) Gillingham, D.; Fei, N., Catalytic X–H insertion reactions based on carbenoids. *Chem. Soc. Rev.* **2013**, *42*, 4918-4931. (g) Davies, H. M. L.; Beckwith, R. E. J., Catalytic Enantioselective C−H Activation by Means of Metal−Carbenoid-Induced C−H Insertion. *Chem. Rev.* **2003**, *103*, 2861-2904. (h) Davies, H. M. L., Finding Opportunities from Surprises and Failures. Development of Rhodium-Stabilized Donor/Acceptor Carbenes and Their Application to Catalyst-Controlled C–H Functionalization. *J. Org. Chem.* **2019**, *84*, 12722-12745. (i) Bulugahapitiya, P.; Landais, Y.; Parra-Rapado, L.; Planchenault, D.; Weber, V., A Stereospecific Access to Allylic Systems Using Rhodium(II)−Vinyl Carbenoid Insertion into Si−H, O−H, and N−H Bonds. *J. Org. Chem.* **1997**, *62*, 1630-1641. (j) Sambasivan, R.; Ball, Z. T., Metallopeptides for Asymmetric Dirhodium Catalysis. *J. Am. Chem. Soc.* **2010**, *132*, 9289-9291. (k) Hunter, A. C.; Chinthapally, K.; Sharma, I., Rh2(esp)2: An Efficient Catalyst for O–H Insertion Reactions of Carboxylic Acids into Acceptor/Acceptor Diazo Compounds. *Eur. J. Org. Chem.* **2016**, *2016*, 2260-2263.

(2) For reviews on dirhodium-catalyzed MCRs involving electrophile capture, see: (a) Guo, X.; Hu, W., Novel Multicomponent Reactions via Trapping of Protic Onium Ylides with Electrophiles. *Acc. Chem. Res.* **2013**, *46*, 2427-2440. (b) Zhang, D.; Hu, W., Asymmetric Multicomponent Reactions Based on Trapping of Active Intermediates. *Chem. Rec.* **2017**, *17*, 739-753. For articles on chiral Brønsted and Lewis acid catalyzed stereoselective reactions, see: (c) Xu, B.; Zhu, S.-F.; Zuo, X.-D.; Zhang, Z.-C.; Zhou, Q.-L., Enantioselective N–H Insertion Reaction of α-Aryl α-Diazoketones: An Efficient Route to Chiral α-Aminoketones. *Angew. Chem., Int. Ed.* **2014**, *53*, 3913-3916. (d) Saito, H.; Morita, D.; Uchiyama, T.; Miyake, M.; Miyairi, S., Cinchona alkaloids induce asymmetry in the insertion reaction of thermally generated carbenes into N−H bonds. *Tetrahedron Lett.* **2012**, *53*, 6662-6664. (e)

Xu, B.; Zhu, S.-F.; Xie, X.-L.; Shen, J.-J.; Zhou, Q.-L., Asymmetric N–H Insertion Reaction Cooperatively Catalyzed by Rhodium and Chiral Spiro Phosphoric Acids. *Angew. Chem., Int. Ed.* **2011**, *50*, 11483-11486. (f) Maolin, Li.; Mengqing, C.; Bin, X.; Shoufei, Z.; Quilin, Z.Enantioselective O—H Bond Insertion of α-Diazoketones with Alcohols Cooperatively Catalyzed by Achiral Dirhodium Complexes and Chiral Spiro Phosphoric Acids. *Acta Chim. Sinica* **2018**, *76*, 883-889. (g) Zhang, Y.; Yao, Y.; He, L.; Liu, Y.; Shi, L., Rhodium(II)/Chiral Phosphoric Acid-Cocatalyzed Enantioselective O–H Bond Insertion of α-Diazo Esters. *Adv. Synth. Catal.* **2017**, *359*, 2754-2761. (h) Tan, F.; Liu, X.; Hao, X.; Tang, Y.; Lin, L.; Feng, X., Asymmetric Catalytic Insertion of α-Diazo Carbonyl Compounds into O–H Bonds of Carboxylic Acids. *ACS Catal.* **2016**, *6*, 6930-6934. (i) Xu, B.; Zhu, S.-F.; Zhang, Z.-C.; Yu, Z.-X.; Ma, Y.; Zhou, Q.-L., Highly enantioselective S–H bond insertion cooperatively catalyzed by dirhodium complexes and chiral spiro phosphoric acids. *Chem. Sci.* **2014**, *5*, 1442-1448. (j) Yang, J.; Ke, C.; Zhang, D.; Liu, X.; Feng, X., Enantioselective Synthesis of 2,2,3-Trisubstituted Indolines via Bimetallic Relay Catalysis of α-Diazoketones with Enones. *Org. Lett.* **2018**, *20*, 4536-4539. For cooperative catalysis of rhodium and other metals, see: (k) Kang, Z.; Chang, W.; Tian, X.; Fu, X.; Zhao, W.; Xu, X.; Liang, Y.; Hu, W., Ternary Catalysis Enabled Three-Component Asymmetric Allylic Alkylation as a Concise Track to Chiral α,α-Disubstituted Ketones. *J. Am. Chem. Soc.* **2021**, *143*, 20818-20827. (l) Chen, Z.-S.; Huang, X.-Y.; Liu, Q.; Song, D.-X.; Yang, F.; Ji, K., Three-component chemo-selective oxy-allylation of α-diazo carbonyl compounds: Access to α-ternary carboxylic esters. *Journal of Catalysis* **2023**, *417*, 52-59. (m) Yuan, W.; Eriksson, L.; Szabó, K. J., Rhodium-Catalyzed Geminal Oxyfluorination and Oxytrifluoro-Methylation of Diazocarbonyl Compounds. *Angew. Chem., Int. Ed.* **2016**, *55*, 8410-8415.

(3) For a review of transition-metal-catalyzed allylic alkylation reactions, see: (a) Trost, B. M.; Crawley, M. L., Asymmetric Transition-Metal-Catalyzed Allylic Alkylations: Applications in Total Synthesis. *Chem. Rev.* **2003**, *103*, 2921-2944. (b) For a review of palladium-catalyzed allylic alkylation reactions, see: Pàmies, O.; Margalef, J.; Cañellas, S.; James, J.; Judge, E.; Guiry, P. J.; Moberg, C.; Bäckvall, J.-E.; Pfaltz, A.; Pericàs, M. A.; Diéguez, M., Recent Advances in Enantioselective Pd-Catalyzed Allylic Substitution: From Design to Applications. *Chem. Rev.* **2021**, *121*, 4373-4505. (c) For a review of rhodium-catalyzed allylic alkylation reactions, see: Thoke, M. B.; Kang, Q., Rhodium-Catalyzed Allylation Reactions. *Synthesis* **2019**, *51*, 2585-2631. (d) Minami, I.; Shimizu, I.; Tsuji, J., Reactions of allylic carbonates catalyzed by palladium, rhodium, ruthenium, molybdenum, and nickel complexes; allylation of carbonucleophiles and decarboxylation- dehydrogenation. *J. Organomet. Chem.* **1985**, *296*, 269-280. For a review of iridium-catalyzed allylic alkylation reactions, see: (e) Cheng, Q.; Tu, H.-F.; Zheng, C.; Qu, J.-P.; Helmchen, G.; You, S.-L., Iridium-Catalyzed Asymmetric Allylic Substitution Reactions. *Chem. Rev.* **2019**, *119*, 1855-1969.

(4) Ma, X.; Jiang, J.; Lv, S.; Yao, W.; Yang, Y.; Liu, S.; Xia, F.; Hu, W., An Ylide Transformation of Rhodium(I) Carbene: Enantioselective Three-Component Reaction through Trapping of Rhodium(I)-Associated Ammonium Ylides by β-Nitroacrylates. *Angew. Chem., Int. Ed.* **2014**, *53*, 13136-13139.

(5) Lu, B.; Liang, X.; Zhang, J.; Wang, Z.; Peng, Q.; Wang, X., Dirhodium(II)/Xantphos-Catalyzed Relay Carbene Insertion and Allylic Alkylation Process: Reaction Development and Mechanistic Insights. *J. Am. Chem. Soc.* **2021**, *143*, 11799-11810.
(6) (a) Davies, H. M. L.; Morton, D., Guiding principles for site selective and stereoselective intermolecular C–H functionalization by donor/acceptor rhodium carbenes. *Chem. Soc. Rev.* **2011**, *40*, 1857-1869. (b) Davies, H. M. L.; Liao, K., Dirhodium tetracarboxylates as catalysts for selective intermolecular C–H functionalization. *Nat. Rev. Chem.* **2019**, *3*, 347-360. (c) Liao, K.; Negretti, S.; Musaev, D. G.; Bacsa, J.; Davies, H. M. L., Site-selective and stereoselective functionalization of unactivated C–H bonds. *Nature* **2016**, *533*, 230-234. (d) DeAngelis, A.; Shurtleff, V. W.; Dmitrenko, O.; Fox, J. M., Rhodium(II)-Catalyzed Enantioselective C−H Functionalization of Indoles. *J. Am. Chem. Soc.* **2011**, *133*, 1650-1653. (e) Li, Z.; Davies, H. M. L., Enantioselective C−C Bond Formation by Rhodium-Catalyzed Tandem Ylide Formation/[2,3]-Sigmatropic Rearrangement between Donor/Acceptor Carbenoids and Allylic Alcohols. *J. Am. Chem. Soc.* **2010**, *132*, 396-401. (f) Davies, H. M. L.; Hansen, T.; Rutberg, J.; Bruzinski, P. R., Rhodium(II) (S)-N-(arylsulfonyl)prolinate catalyzed asymmetric insertions of vinyl- and phenylcarbenoids into the Si–H bond. *Tetrahedron Lett.* **1997**, *38*, 1741-1744. (g) Zhou, C.-Y.; Wang, J.-C.; Wei, J.; Xu, Z.-J.; Guo, Z.; Low, K.–H.; Che, C.-M., Dirhodium Carboxylates Catalyzed Enantioselective Coupling Reactions of α-Diazophosphonates, Anilines, and Electron-Deficient Aldehydes. *Angew. Chem., Int. Ed.* **2012**, *51*, 11376-11380.
(7) (a) Trindade, A. F.; Coelho, J. A. S.; Afonso, C. A. M.; Veiros, L. F.; Gois, P. M. P., Fine Tuning of Dirhodium(II) Complexes: Exploring the Axial Modification. *ACS Catal.* **2012**, *2*, 370-383. (b) Hong, B.; Shi, L.; Li, L.; Zhan, S.; Gu, Z., Paddlewheel dirhodium(II) complexes with N-heterocyclic carbene or phosphine ligand: New reactivity and selectivity. *Green Synthesis and Catalysis* **2022**, *3*, 137-149. (c) Sambasivan, R.; Zheng, W.; Burya, S. J.; Popp, B. V.; Turro, C.; Clementi, C.; Ball, Z. T., A tripodal peptide ligand for asymmetric Rh(ii) catalysis highlights unique features of on-bead catalyst development. *Chem. Sci.* **2014**, *5*, 1401-1407. (d) Sarkar, M.; Daw, P.; Ghatak, T.; Bera, J. K., Amide-Functionalized Naphthyridines on a RhII–RhII Platform: Effect of Steric Crowding, Hemilability, and Hydrogen-Bonding Interactions on the Structural Diversity and Catalytic Activity of Dirhodium(II) Complexes. *Chem. Eur. J.* **2014**, *20*, 16537-16549. (e) Anderson, B. G.; Cressy, D.; Patel, J. J.; Harris, C. F.; Yap, G. P. A.; Berry, J. F.; Darko, A., Synthesis and Catalytic Properties of Dirhodium Paddlewheel Complexes with Tethered, Axially Coordinating Thioether Ligands. *Inorg. Chem.* **2019**, *58*, 1728-1732. (f) Cressy, D.; Zavala, C.; Abshire, A.; Sheffield, W.; Darko, A., Tuning Rh(II)-catalysed cyclopropanation with tethered thioether ligands. *Dalton Transactions* **2020**, *49*, 15779-15787. (g) Zavala, C.; Darko, A., Effect of Tethered, Axially Coordinated Ligands (TACLs) on Dirhodium(II,II) Catalyzed Cyclopropanation: A Linear Free Energy Relationship Study. *J. Org. Chem.* **2022**, *87*, 6910-6917. (h) Laconsay, C. J.; Pla-Quintana, A.; Tantillo, D. J., Effects of Axial Solvent Coordination to Dirhodium Complexes on the Reactivity and Selectivity in C–H Insertion Reactions: A Computational Study. *Organometallics* **2021**, *40*, 4120-4132.
(8) (a) Yang, Y.; Lu, B.; Xu, G.; Wang, X., Overcoming O–H Insertion to Para-Selective C–H Functionalization of Free Phenols: Rh(II)/Xantphos Catalyzed Geminal Difunctionalization of Diazo Compounds. *ACS Cent. Sci.* **2022**, *8*, 581-589. (b) Zhang, J.; Lu, B.; Ge, Z.; Wang,

L.; Wang, X., Selective Construction of All-Carbon Quaternary Centers via Relay Catalysis of Indole C–H Functionalization/Allylic Alkylation. *Org. Lett.* **2022**, *24*, 8423-8428. (c) Ge, Z.; Lu, B.; Teng, H.; Wang, X., Efficient Synthesis of Diaryl Quaternary Centers by Rh(II)/Xantphos Catalyzed Relay C−H Functionalization and Allylic Alkylation. *Chem. Eur. J.* **2023**, *29*, e202202820.
(9) Shi, L.; Xue, X.; Hong, B.; Li, Q.; Gu, Z., Dirhodium(II)/Phosphine Catalyst with Chiral Environment at Bridging Site and Its Application in Enantioselective Atropisomer Synthesis. *ACS Cent. Sci.* 2023. https://doi.org/10.1021/acscentsci.2c01207
(10) Pirrung, M. C.; Liu, H.; Morehead, A. T., Rhodium Chemzymes: Michaelis−Menten Kinetics in Dirhodium(II) Carboxylate-Catalyzed Carbenoid Reactions. *J. Am. Chem. Soc.* **2002**, *124*, 1014-1023.
(11) The reaction catalysed by D7 was earlier to have a reduced rate and was thus not taking into consideration as the active catalytic species.
(12) The bipyridine analogue of this complex is well known: (a) Perlepes, S. P.; Huffman, J. C.; Matonic, J. H.; Dunbar, K. R.; Christou, G., Binding of 2,2'-bipyridine to the dirhodium(II) tetraacetate core: unusual structural features and biological relevance of the product Rh2(OAc)4(bpy). *J. Am. Chem. Soc.* **1991**, *113*, 2770-2771. (b) Crawford, C. A.; Matonic, J. H.; Streib, W. E.; Huffman, J. C.; Dunbar, K. R.; Christou, G., Reaction of 2,2'-bipyridine (bpy) with dirhodium carboxylates: mono-bpy products with variable chelate binding modes and insights into the reaction mechanism. *Inorg. Chem.* **1993**, *32*, 3125-3133. (c) Esteban, J.; Estevan, F.; Sanaú, M., Analysis of the main structural trends for biscyclometalated dinuclear rhodium compounds with nitrogen donor axial ligands. *Inorganica Chimica Acta* **2009**, *362*, 1179-1184. (d) Ćwikowska, M.; Pruchnik, F. P.; Starosta, R.; Chojnacki, H.; Wilczok, A.; Ułaszewski, S., Dinuclear Rh(II) complexes with one polypyridyl ligand, structure, properties and antitumor activity. *Inorganica Chimica Acta* **2010**, *363*, 2401-2408.
(13) (a) Hansen, J.; Autschbach, J.; Davies, H. M. L., Computational Study on the Selectivity of Donor/Acceptor-Substituted Rhodium Carbenoids. *J. Org. Chem.* **2009**, *74*, 6555-6563. (b) Liang, Y.; Zhou, H.; Yu, Z.-X., Why Is Copper(I) Complex More Competent Than Dirhodium(II) Complex in Catalytic Asymmetric O−H Insertion Reactions? A Computational Study of the Metal Carbenoid O−H Insertion into Water. *J. Am. Chem. Soc.* **2009**, *131*, 17783-17785. (c) Zhou, M.; Springborg, M., Theoretical study of the mechanism behind the site- and enantio-selectivity of C–H functionalization catalysed by chiral dirhodium catalyst. *Phys. Chem. Chem. Phys.* **2020**, *22*, 9561-9572.
(14) (a) Bastos, E. L., Acid–Base and Solvation properties of Metal Enolates. Part 1: The Enolate Ion and Main-Group Metal Enolates. In *PATAI'S Chemistry of Functional Groups*, **2017**, pp 1-54. (b) Olmstead, W. N.; Bordwell, F. G., Ion-pair association constants in dimethyl sulfoxide. *J. Org. Chem.* **1980**, *45*, 3299-3305.
(15) (a) Dijkstra, G.; Kruizinga, W. H.; Kellogg, R. M., An assessment of the causes of the "cesium effect". *J. Org. Chem.* **1987**, *52*, 4230-4234. (b) Kennedy, C. R.; Guidera, J. A.; Jacobsen, E. N., Synergistic Ion-Binding Catalysis Demonstrated via an Enantioselective, Catalytic [2,3]-Wittig Rearrangement. *ACS Cent. Sci.* **2016**, *2*, 416-423.
(16) See Figure S4 for the calculated reaction profile for the formation of the κ^2-Xantphos dirhodium tetracarboxylate active catalyst **D4** and the complete dissociation of the octanoate

ligand from **D4** followed along with the concomitant association of the allyl carbonate to form **E**.
(17) (a) Lou, Y.; Horikawa, M.; Kloster, R. A.; Hawryluk, N. A.; Corey, E. J., A New Chiral Rh(II) Catalyst for Enantioselective [2 + 1]-Cycloaddition. Mechanistic Implications and Applications. *J. Am. Chem. Soc.* **2004**, *126*, 8916-8918. (b) Lou, Y.; Remarchuk, T. P.; Corey, E. J., Catalysis of Enantioselective [2+1]-Cycloaddition Reactions of Ethyl Diazoacetate and Terminal Acetylenes Using Mixed-Ligand Complexes of the Series Rh2(RCO2)n (L*4-n). Stereochemical Heuristics for Ligand Exchange and Catalyst Synthesis. *J. Am. Chem. Soc.* **2005**, *127*, 14223-14230. (c) Wang, C.; Zhou, Y.; Bao, X., Mechanistic Insights into the Rh-Catalyzed Transannulation of Pyridotriazole with Phenylacetylene and Benzonitrile: A DFT Study. *J. Org. Chem.* **2017**, *82*, 3751-3759.
(18) Nowlan, D. T.; Singleton, D. A., Mechanism and Origin of Enantioselectivity in the Rh2(OAc)(DPTI)3-Catalyzed Cyclopropenation of Alkynes. *J. Am. Chem. Soc.* **2005**, *127*, 6190-6191.
(19) Liu, Z.; Patel, C.; Harvey, J. N.; Sunoj, R. B., Mechanism and reactivity in the Morita–Baylis–Hillman reaction: the challenge of accurate computations. *Phys. Chem. Chem. Phys.* **2017**, *19*, 30647-30657.
(20) Plata, R. E.; Singleton, D. A., A Case Study of the Mechanism of Alcohol-Mediated Morita Baylis–Hillman Reactions. The Importance of Experimental Observations. *J. Am. Chem. Soc.* **2015**, *137*, 3811-3826.
(21) See Table S1 and Table S2 for a comparision of the gas phase and solvent phase optimized separated ion pair (**E**) energy at different levels of theory.
(22) (a) Evans, P. A.; Nelson, J. D., Conservation of Absolute Configuration in the Acyclic Rhodium-Catalyzed Allylic Alkylation Reaction: Evidence for an Enyl ($\sigma + \pi$) Organorhodium Intermediate. *J. Am. Chem. Soc.* **1998**, *120*, 5581-5582. (b) Lawson, D. N.; Osborn, J. A.; Wilkinson, G., Interaction of tris(triphenylphosphine)chlororhodium(I) with iodomethane, methylallyl, and allyl chloride. *J. Chem. Soc. A* **1966**, 1733-1736. (c) Turnbull, B. W. H.; Evans, P. A., Asymmetric Rhodium-Catalyzed Allylic Substitution Reactions: Discovery, Development and Applications to Target-Directed Synthesis. *J. Org. Chem.* **2018**, *83*, 11463-11479.
(23) Zhu, T. P.; Ahsan, M. Q.; Malinski, T.; Kadish, K. M.; Bear, J. L., Electrochemical studies of a series of dirhodium(II) complexes with acetate and acetamidate bridging ligands. *Inorg. Chem.* **1984**, *23*, 2-3.
(24) (a) van Haaren, R. J.; Zuidema, E.; Fraanje, J.; Goubitz, K.; Kamer, P. C. J.; van Leeuwen, P. W. N. M.; van Strijdonck, G. P. F., Synthesis and characterisation of bite angle-dependent (η1-allyl)Rh and (η3-allyl)Rh complexes bearing diphosphine ligands. Implications for nucleophilic substitution reactions. *C. R. Chimie* **2002**, *5*, 431-440. (b) Tsuji, J.; Minami, I.; Shimizu, I., Allyation of carbonucleophiles with allylic carbonates under neutral conditions catalyzed by rhodium complexes. *Tetrahedron Lett.* **1984**, *25*, 5157-5160.
(25) Pareek, M.; Sunoj, R. B., Mechanistic insights into rhodium-catalyzed enantioselective allylic alkylation for quaternary stereogenic centers. *Chem. Sci.* **2021**, *12*, 2527-2539.
(26) *Gaussian 16, Revision C.01*, Frisch, M. J., Trucks, G. W., Schlegel, H. B., Scuseria, G. E., Robb, M. A., Cheeseman, J. R., Scalmani, G., Barone, V., Petersson, G. A., Nakatsuji, H., Li, X., Caricato, M., Marenich, A. V., Bloino, J., Janesko, B. G., Gomperts, R., Mennucci, B.,

Hratchian, H. P., Ortiz, J. V., Izmaylov, A. F., Sonnenberg, J. L., Williams-Young, D., Ding, F., Lipparini, F., Egidi, F., Goings, J., Peng, B., Petrone, A., Henderson, T., Ranasinghe, D., Zakrzewski, V. G., Gao, J., Rega, N., Zheng, G., Liang, W., Hada, M., Ehara, M., Toyota, K., Fukuda, R., Hasegawa, J., Ishida, M., Nakajima, T., Honda, Y., Kitao, O., Nakai, H., Vreven, T., Throssell, K., Montgomery, J. A., Jr., Peralta, J. E., Ogliaro, F., Bearpark, M. J., Heyd, J. J., Brothers, E. N., Kudin, K. N., Staroverov, V. N., Keith, T. A., Kobayashi, R., Normand, J., Raghavachari, K., Rendell, A. P., Burant, J. C., Iyengar, S. S., Tomasi, J., Cossi, M., Millam, J. M., Klene, M., Adamo, C., Cammi, R., Ochterski, J. W., Martin, R. L., Morokuma, K., Farkas, O., Foresman, J. B., Fox, D. J. Gaussian, Inc., Wallingford CT, **2016.**

(27) (a) Becke, A. D., Density-functional thermochemistry. III. The role of exact exchange. *J. Chem. Phys.* **1993**, *98*, 5648-5652. (b) Lee, C.; Yang, W.; Parr, R. G., Development of the Colle-Salvetti correlation-energy formula into a functional of the electron density. *Phys. Rev. B* **1988**, *37*, 785-789.

(28) (a) Hariharan, P. C.; Pople, J. A., The influence of polarization functions on molecular orbital hydrogenation energies. *Theoret. Chim. Acta* **1973**, *28*, 213-222. (b) Hehre, W. J.; Ditchfield, R.; Pople, J. A., Self—Consistent Molecular Orbital Methods. XII. Further Extensions of Gaussian—Type Basis Sets for Use in Molecular Orbital Studies of Organic Molecules. *J. Chem. Phys.* **1972**, *56*, 2257-2261.

(29) (a) Andrae, D.; Häußermann, U.; Dolg, M.; Stoll, H.; Preuß, H., Energy-adjusted ab initio pseudopotentials for the second and third row transition elements. *Theoret. Chim. Acta* **1990**, *77*, 123-141. (b) Fuentealba, P., On the reliability of semiempirical pseudopotentials: dipole polarisability of the alkali atoms. *J. Phys. B: Atom. and Mol. Phys.* **1982**, *15*, L555.

(30) Grimme, S., Ehrlich, S.; Goerigk, L., *J. Comput. Chem*. **2011**, *32*, 1456-1465.

(31) Marenich, A. V.; Cramer, C. J.; Truhlar, D. G., Universal Solvation Model Based on Solute Electron Density and on a Continuum Model of the Solvent Defined by the Bulk Dielectric Constant and Atomic Surface Tensions. *J. Phys. Chem. B* **2009**, *113*, 6378-6396.

(32) Wang, Y.; Zhu, Y.; Chen, Z.; Mi, A.; Hu, W.; Doyle, M. P., A Novel Three-Component Reaction Catalyzed by Dirhodium(II) Acetate: Decomposition of Phenyldiazoacetate with Arylamine and Imine for Highly Diastereoselective Synthesis of 1,2-Diamines. *Org. Lett.* **2003**, *5*, 3923-3926.